ELSEVIER

Chemical Engineering Journal 88 (2002) 111–118

Chemical Engineering Journal

www.elsevier.com/locate/cej

Measurement of gas hold-up in bubble columns from low frequency acoustic emissions

Jonathan W.R. Boyd*, Julie Varley

Department of Chemical Engineering and Chemical Technology, Imperial College of Science, Technology and Medicine, Prince Consort Road, London SW7 2BY, UK

Received 21 May 2001; received in revised form 12 November 2001; accepted 12 November 2001

Abstract

This paper demonstrates a novel method of global gas hold-up estimation in a laboratory scale bubble column using acoustic emissions from within the column, which are caused by bubble generation. Bubble formation excites the column to resonate at its natural frequencies; these frequencies are determined by the vessel dimensions. Peaks in the 0–1000 Hz range of the acoustic spectrum were observed and identified as the column resonance frequencies. Measured changes in resonance frequencies for a range of global gas hold-ups (up to 20%) correlated well with theory. This method of global gas hold-up monitoring should be particularly useful for systems where measurements of changes in liquid height are not possible.

Keywords: Bubble columns; Acoustic emissions; Gas hold-up

1. Introduction

Bubble columns are used in many chemical engineering processes to mix a gas with a liquid, for example in bioreactors. Accurate knowledge of gas hold-up and bubble size within a bubble column is necessary for understanding and predicting mass transfer for optimal operation. Several techniques exist to measure gas hold-up either globally throughout the vessel or as a function of position. The simplest method of measuring the global gas hold-up within a vessel is to measure the change in dispersion height due to the presence of the gas bubbles [1]. However, application of this technique is limited because a transparent vessel is required and the accuracy of liquid height measurement is poor when foaming occurs or when there are large fluctuations in the liquid level. Measuring the difference in pressure between two levels within a column is another method used to measure global gas hold-up but pressure tappings can be subject to fouling in real systems [1]. Probe techniques, using conductivity measurement [2], for example, have been developed to measure the spatial distribution of gas hold-up but again these can be subject to fouling. To avoid intrusion into the process tomographic techniques using an array of impedance or conductivity probes arranged on the inside of the vessel wall can be used to measure gas hold-up throughout the cross section of the vessel, e.g. Veera and Joshi [3] and Schmitz and Mewes [4].

The presence of bubbles in water has been shown to affect the attenuation and speed of a propagating sound wave and such effects have been used to measure gas hold-up within a dispersion by actively generating an ultrasonic wave and measuring how this wave is affected by the presence of bubbles [5]. Tomographic techniques using ultrasound are also being developed allowing the spatial changes in gas hold-up to be mapped-out throughout a vessel [6]. The velocity of sound within a gas–solid fluidised bed was investigated by Roy et al. [7] using two different methods. Firstly, the fluidised bed was subjected to a sudden, vertical impulse (lifting and dropping the column!). The measured frequency of the damped pressure fluctuations with time was related to the void fraction. Secondly, Roy et al. [7] cross-correlated the signals from two pressure probes above and below an acoustic event (bubble formation artificially introduced into the system mid-way up the column) to estimate the speed of sound in the column. Costigan and Whalley [8] related the speed of a sound wave propagating in bubbly air–water flow in a pipe with the gas void fraction. A transient acoustic wave was created by closing a valve at one end that propagated up and down the pipe. The time between peaks in the measured pressure signal was taken to be the time for the wave to propagate to the top of the pipe and back; this was used to estimate

* Corresponding author. Tel.: +44-(0)20-75895111x55686; fax: +44-(0)20-75945604.
E-mail address: j.boyd@ic.ac.uk (J.W.R. Boyd).

1385-8947/02/$ – see front matter
PII: S1385-8947(01)00297-2

Nomenclature

a	radius of a bubble (m)
a_n	constant of proportionality used in Eq. (12)
c_m	speed of sound in the gas–liquid mixture ($m\,s^{-1}$)
h_0	ungassed height of liquid above the sparger (m)
H	overall height of the dispersion (m)
p_0	ambient pressure (Pa)
R	radius of the bubble column vessel (m)
β	gas voidage (%)
γ	ratio of specific heats
λ_n	wavelength of mode n (m)
ρ_l	density of liquid ($kg\,m^{-3}$)

the speed of sound, which was then related to the void fraction.

Although the techniques of both Roy et al. [7] and Costigan and Whalley [8] did not involve the active generation of sound by means of a transducer, the sound waves created were still not natural to the processes under investigation and, therefore, not suitable techniques for the monitoring of gas hold-up without extensive disruption to the process. Passive acoustic emission monitoring involves the measurement of sound created by the process itself to ascertain process information [9]. This investigation demonstrates that the passive measurement of acoustic emissions, created naturally by sparging gas in to a laboratory bubble column can be used to measure the global gas hold-up within a dispersion. The frequency of peaks in the acoustic spectrum measured inside the column has been correlated with the gas hold-up.

2. Theory

Acoustic emissions from gas bubbles in liquid have mainly been investigated to establish the cause of ambient oceanic sound. Sound above 1 kHz is caused by the volume pulsations of bubbles when they are entrained below the surface, which results in an exponentially damped acoustic pulse. The frequency of the pulse, f_B is related to bubble size according to [10,11]

$$f_B = \frac{1}{2\pi a}\sqrt{\frac{3\gamma p_0}{\rho_l}} \tag{1}$$

where a is the radius of the bubble, p_0 the surrounding ambient pressure, γ the specific heat ratio and ρ_l the density of the liquid. For an air bubble in water Eq. (1) approximates to

$$f_B = \frac{3.2}{a} \tag{2}$$

A bubble of radius 3 mm would therefore emit a pulse of around 1 kHz based on Eq. (2). This equation has been used to size bubbles in chemical engineering applications [12].

Oceanic sound, at frequencies below 1 kHz, is believed to be caused by the collective oscillations of bubble clouds [13–16]. Bubble formation noise excites a standing wave in the cloud of bubbles. The frequencies associated with these standing waves depend on the scale, geometry and the void fraction within the cloud. The average pressure field, P, inside a gas–liquid bubbly mixture was described by solution of the Helmholtz equation [14]

$$\nabla^2 P + k_m^2(P - p_0) = 0 \tag{3}$$

where k_m is a constant called the wavenumber.

Within a cylindrical tube, excited into resonance, several modes or frequencies of resonance can occur simultaneously. In the case of a thin cylindrical column, for which the diameter is much smaller than the wavelength, the standing waves can be regarded as one-dimensional plane waves, which propagate along the tube's length [17].

The frequency of the standing wave depends on the boundary conditions at the surfaces within the tube. At a pressure release surface or opening, the acoustic pressure is zero and at a totally rigid boundary the vibrating particles have zero velocity.

In a column of liquid inside a tube the surface of the liquid can be regarded as a pressure release boundary. If the

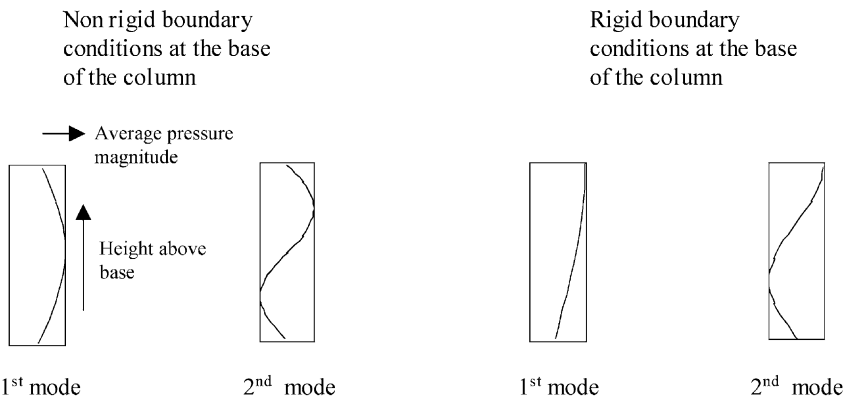

Fig. 1. Representation of the pressure variation in the axial direction for the first two resonance modes within an open ended column for both the rigid and non-rigid boundary conditions at its base.

base of the column is regarded as rigid then the lower order modal frequencies in the column are [14]

$$f_n = \frac{(2n-1)c_m}{4H}, \quad n = 1, 2, 3, \ldots \tag{4}$$

where c_m is the speed of sound in the gas–liquid mixture and H the height of the gas–liquid mixture given by

$$H = \frac{h_0}{1 - (\beta/100)} \tag{5}$$

where β is the void fraction or gas hold-up and h_0 the initial liquid height.

A pressure release boundary (i.e. non-rigid) at the base of the column would result in the lower order modal frequencies being

$$f_n = \frac{nc_m}{2H}, \quad n = 1, 2, 3, \ldots \tag{6}$$

Fig. 1 shows representations of the pressure variations of the first two modes of resonance within a column for rigid and non-rigid boundary conditions at the base in the axial direction. In reality the boundary conditions at the base of the vessel will behave somewhere between the pressure release and the rigid boundary condition depending on the materials used to construct the column.

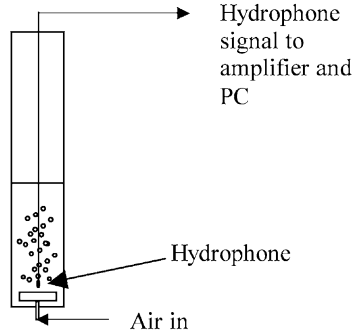

Fig. 2. Diagram of the experimental set-up.

For low sound frequencies and assuming isothermal conditions the speed of sound inside the bubbly mixture can be estimated from [18]

$$c_m^2 = \frac{\gamma p_0}{(\beta/100)(1-\beta/100)\rho_l} \tag{7}$$

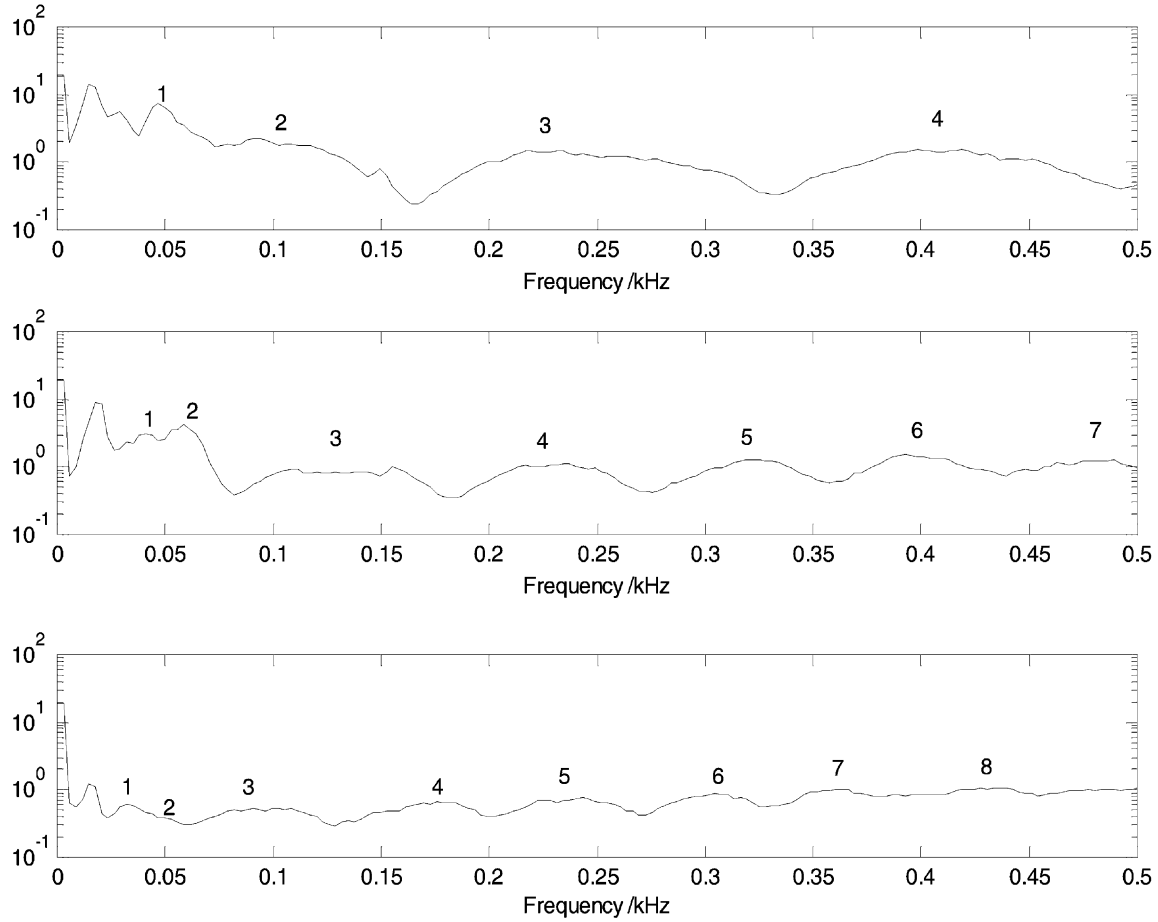

Fig. 3. The effect of increasing gas flow rate (0.013, 0.021 and 0.0042 m s^{-1}) on the acoustic emission spectrum measured just above the sparger in the 0–0.5 kHz range. The peaks are marked in the numerical order in which they appear in the spectrum.

where c_m is the speed of sound in the bubbly mixture and γ the specific heat ratio which is equal to 1.

For cylinders of larger diameters relative to the acoustic wavelength, higher order modes can exist where the non-plane waves can propagate within the column. The frequency of these waves again depends on the boundary conditions at the tube wall itself. The two extreme conditions are again a pressure release boundary or rigid boundary.

3. Experimental

Fig. 2 shows a diagram of the bubble column system. Air was sparged into a column 0.075 m diameter, 0.8 m glass column. The base of the column consisted of a large rubber bung into which two types of sparger could be sealed. Sparger A consisted of a sintered gas disc of porosity 3 and 30 mm diameter and positioned at a height of 15 mm above the column base. Sparger B was a porous plastic disc 65 mm in diameter, sealed into a plastic filter funnel, the top of which was 70 mm above the column base. Compressed air was sparged into the vessel at flow rates up to 12 l min^{-1} (corresponding to superficial gas velocities of up to 0.05 m s^{-1}). The column was filled with liquid to various heights above the top of the sparger (0.2, 0.3, 0.45 and 0.6 m). De-ionised water was used as the liquid inside the column. Gas hold-up was measured from the change in liquid height due to the presence of the gas. For sparger A, the heterogeneous flow regime occurred at superficial gas velocities of around 0.02 m s^{-1}, which caused the liquid surface to fluctuate violently making the measurement of the dispersion height very approximate (±20 mm). Better accuracy was obtainable using sparger B for which the change in height of the dispersion could be estimated to within 1 mm for the lowest low rates used and within 5 mm at the highest flow rates (the heterogeneous regime was not attained for this sparger) and the liquid height therefore remained steady.

A 8301 Bruel and Kjaer hydrophone attached to a rod was used to measure the acoustic emissions from at various heights along the central axis of the bubble column. The signal from the hydrophone was amplified using a Bruel and Kjaer Nexus pre-amplifier and sent directly to a PC where the signal was acquired at a rate of 1000 or 3000 samples/s using an NI 4551 dynamic signal analyser card (National Instruments, Newbury) and LabVIEW software. The sampling rate was chosen to produce a spectrum containing the maximum number of spectral peaks and with the most suitable resolution. MATLAB or Excel software was then used for further spectral analysis of the signal in the frequency range 0–1000 Hz.

4. Results and discussion

In Fig. 3, the low frequency sound spectrum (0–0.5 kHz) measured at the centre of the column just above the sparger

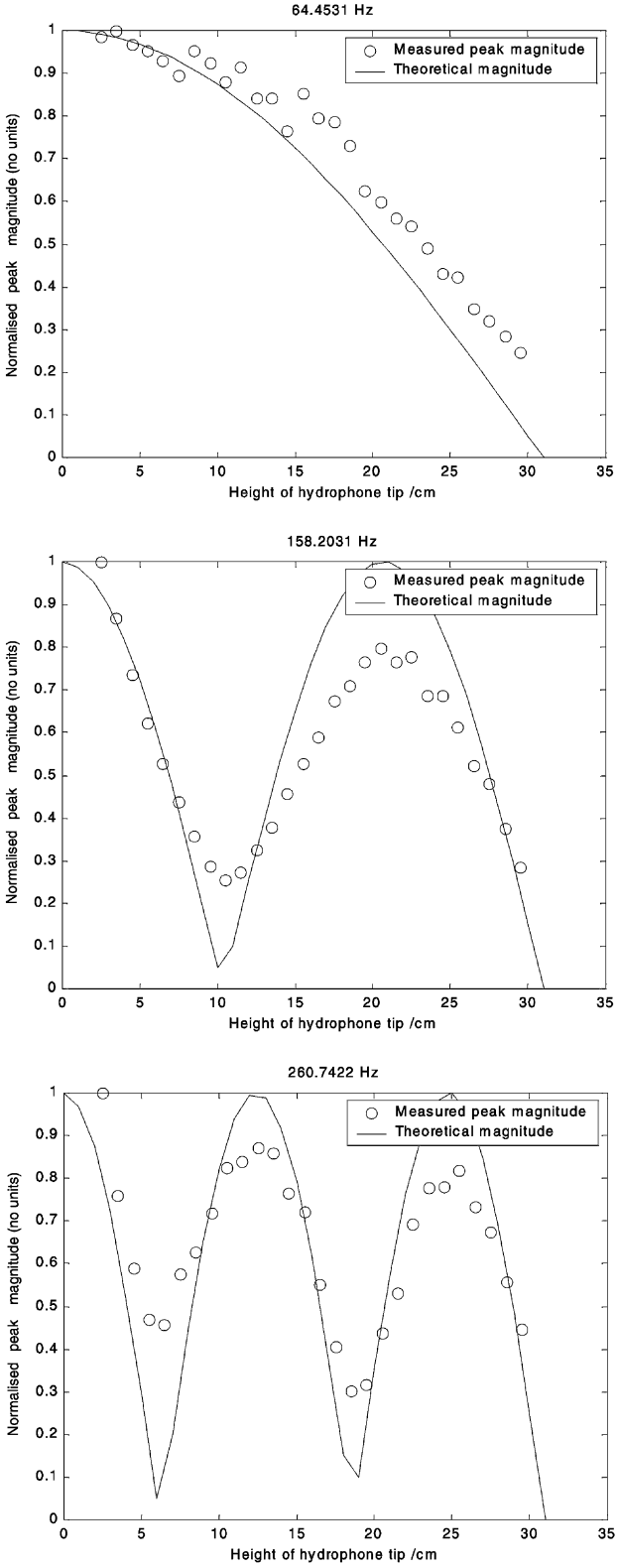

Fig. 4. Variation in the spectral magnitude with height from base at frequencies where peaks appear in the spectra measured just above the sparger (sparger B, $h_0 = 0.31$ cm). The theoretical curves for the magnitude variation with height assuming rigid base conditions are plotted as unbroken lines.

for gas flow rates of 1, 3 and 5 l min^{-1} (corresponding to superficial gas flow rates of 0.013, 0.021 and 0.0042 m s^{-1}, respectively) sparged into de-ionised water are shown. The ungassed liquid height was 31 cm above the base of the column. Peaks in the spectrum are marked in the numerical order they appear in the spectrum. Increasing the gas flow rate into the column resulted in a shifting of peaks to lower frequencies. The increased gas flow rate and gas hold-up also resulted in a decrease in the magnitude of the peaks.

Fig. 4(a)–(c) shows how the magnitude (normalised in each case to the maximum pressure magnitude in the spectrum) at frequencies corresponding to the first three peaks in the spectrum measured just above the sparger, varied with the measurement height for the case. The gas superficial velocity was 0.0075 m s^{-1}, the original liquid height was 0.31 m and sparger B was used. Theoretical curves (unbroken lines) assuming a rigid base calculated using the following equation are also plotted for comparison:

$$p_{\text{norm}} = \cos\left(\frac{2n-1}{4H}\right)h, \quad n = 1, 2, 3, \ldots \tag{8}$$

where p_{norm} is the pressure magnitude normalised by the maximum peak pressure and h the height above the base. There is a reasonable agreement between the theoretical and experimental curves.

Substituting Eqs. (5) and (7) into Eq. (4) which assumes rigid boundary conditions at the base of the column allows the theoretical resonance frequencies to be calculated from

$$f_n = \frac{2n-1}{4h_0}\left(\frac{\gamma p_0(1-\beta/100)}{(\beta/100)\rho_{\text{l}}}\right)^{1/2}, \quad n = 1, 2, 3, \ldots \tag{9}$$

where f_n is the frequency of the nth peak.

Fig. 5 shows how the theoretical resonance frequencies, calculated using Eq. (9), vary with gas hold-up for an initial liquid height of 0.31 m. For comparison the experimentally measured peak frequencies at various gas hold-ups are also plotted in Fig. 5. The theoretical peak frequency calculated assuming a rigid base to the column under-predicted the actual measured values throughout the range of gas hold-ups investigated. However, the variation of the measured peak frequency with gas hold-up did follow the same pattern as the theoretical predictions. Continuing with the assumption that the base of the column is rigid then the gas hold-up can be estimated by rearranging Eq. (9) to give

$$\beta = 100 \times \frac{\gamma p_0(2n-1)^2}{16 f_n{}^2 h_0^2 \rho_{\text{l}} + \gamma p_0(2n-1)^2}, \quad n = 1, 2, 3, \ldots \tag{10}$$

The variation of the gas hold-up estimated from the change in dispersion height and the gas hold-up estimated from the acoustic spectrum using Eq. (10) with the superficial gas velocities for sparger B are shown in Fig. 6 for an initial liquid height of 0.31 cm. The error bars in the

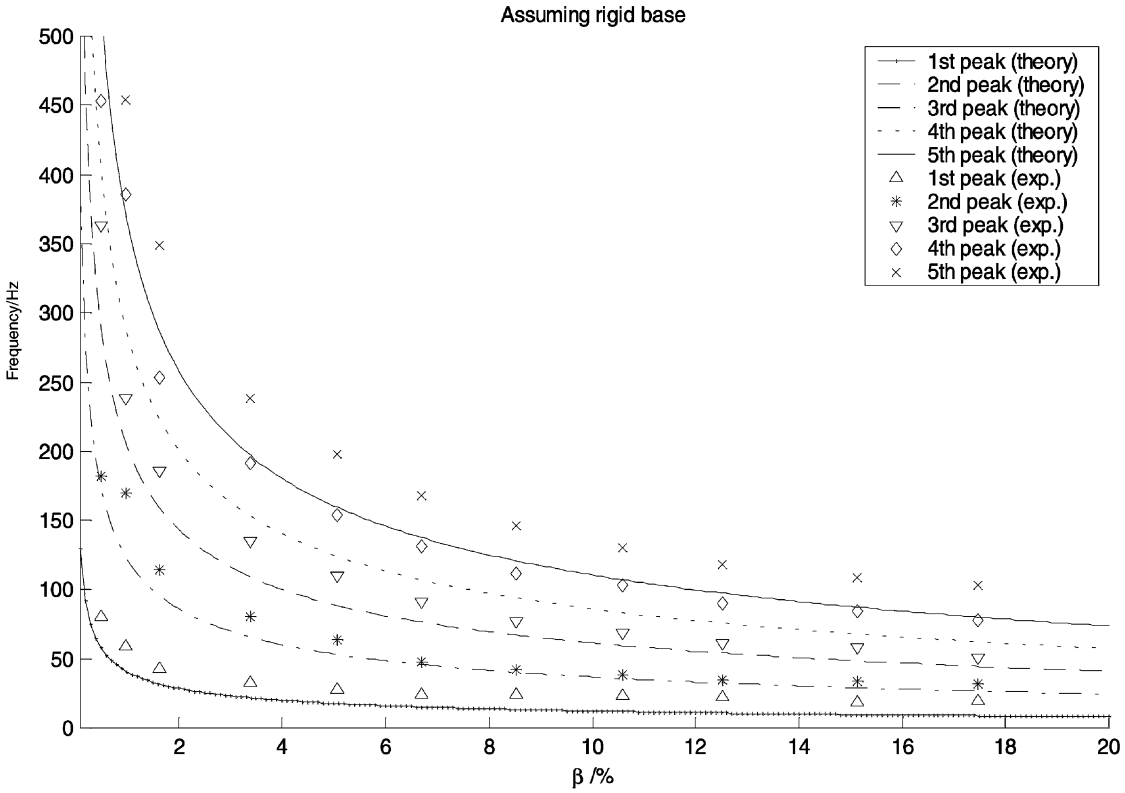

Fig. 5. Variation in spectral peak frequencies measured just above the sparger with measured gas hold-up. Also included in the diagram are the theoretical frequencies assuming rigid boundary conditions at the base of the column calculated from Eq. (8) (sparger B, $h_0 = 0.31$ cm).

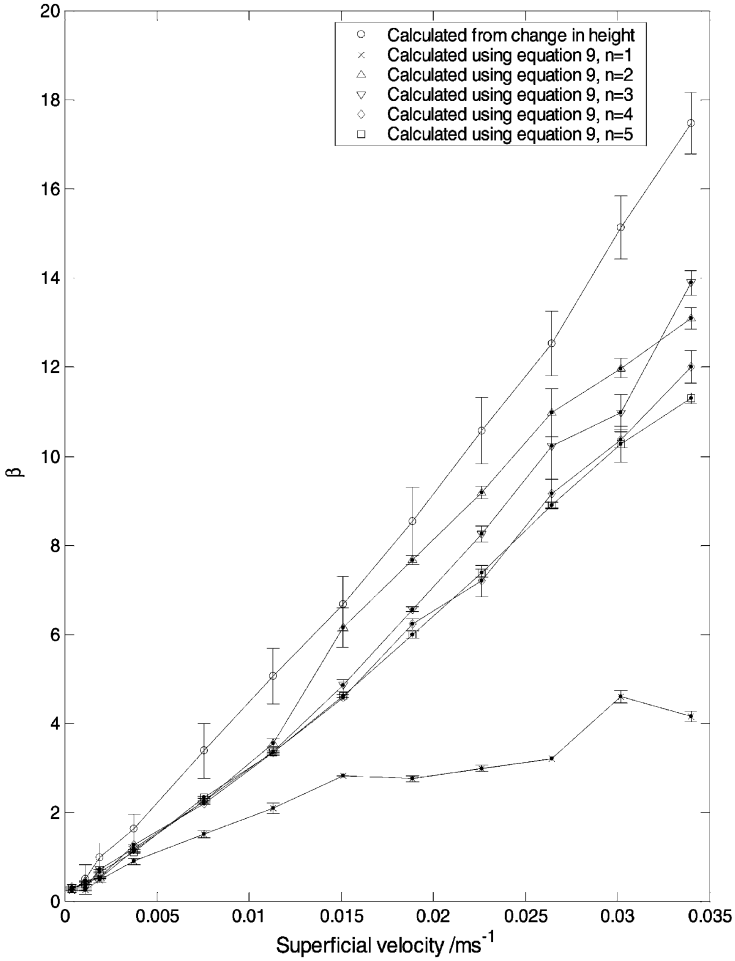

Fig. 6. The variation of estimated gas hold-up from the measured peak frequencies assuming rigid boundary conditions at the base of the column and the actual gas hold-up with superficial gas velocity (sparger B, $h_0 = 0.31$ cm).

diagram for the acoustically estimated gas hold-up are based on one standard deviation of five acoustic spectra. The error bars for the gas hold-up measured from the change in the dispersion height indicate the estimated error in the height measurement (described in Section 3). The gas hold-up was underestimated by between 30 and 50% for all the resonance modes except the 1st mode. The gas hold-up estimated from the 1st mode frequency is less sensitive to changes at high gas hold-ups. Similar results were found with sparger A but are not presented here as the gas hold-up measurement from the change in the dispersion height became increasingly inaccurate in the heterogeneous regime. It was noted, however, that the transition to the heterogeneous regime was marked by a deviation from linear relationship between the acoustically estimated gas hold-up and superficial gas velocity, which would be expected for the heterogeneous regime [1]. The correlation coefficient between the acoustically estimated gas hold-ups from the frequencies of the 2nd to 5th modes and the gas hold-up estimated from the change in dispersion height is between 0.95 and 0.99 demonstrating an excellent correlation between the peak frequencies and the gas hold-up within the dispersion. This good correlation suggests that the column base was not completely rigid, i.e.

$$\tfrac{1}{4}(2n-1) < \lambda_n < \tfrac{1}{2}n, \quad n = 1, 2, 3, \ldots \tag{11}$$

where λ_n is the wavelength of the standing wave. If it assumed that the wavelength of the sound waves is proportional to the dispersion height then

$$\lambda_n = a_n \frac{h_0}{1 - (\beta/100)} \tag{12}$$

where a_n is a constant of proportionality for the nth peak in the low frequency acoustic spectrum.

Combining Eqs. (5), (7) and (12), the frequency of a modal peak in the spectrum would result in

$$f_n^2 = \left(\frac{1}{a_n}\right)^2 \left(\frac{p_0}{\rho_l h_0^2}\right) \left(\frac{1 - (\beta/100)}{\beta/100}\right) \tag{13}$$

From plots of f_n^2 against $(p_0/\rho_l h_0^2)(1 - (\beta/100)/(\beta/100))$ the values of a_n were estimated for the various experimental conditions. These are shown in Table 1 for sparger B with tap

Table 1
Experimental values of a_n

Initial liquid height above sparger (m)	a_n (theoretical value assuming rigid boundary at the base in brackets)				
	a_1 (0.25)	a_2 (0.75)	a_3 (1.25)	a_4 (1.75)	a_5 (2.25)
0.2	0.37	0.96	1.57	2.01	2.61
0.3	0.32	1.1	1.69	2.30	3.14
0.6	0.35	0.85	1.54	2.03	2.61
Average	0.34	0.97	1.6	2.12	2.77

water. All the constants were slightly above those expected for a rigid base.

Fig. 7 shows the parity plot of gas hold-up estimated from the 2nd to 5th modal peaks in the spectrum calculated using the average a_n values shown in Table 1 and the measured gas hold-up from the change in height of the dispersion for all the conditions used in the study. The 1st modal peak has not been used because the changes in frequency for this mode were not sensitive enough to changes in the gas hold-up. The correlation coefficient is 0.91 for the range of gas hold-ups considered in these experiments.

In these studies, the acoustic emissions from a laboratory scale bubble column have been shown to correlate well with changes in the gas hold-up. For situations where measurement of the liquid dispersion height is not possible this could provide an uncomplicated method of monitoring global gas hold-up. Indeed, it may be possible to make the measurements from outside the vessel making the technique completely non-intrusive to the process.

It is useful to consider the effects of increasing scale. For the size of bubble column studied here, it was the lower modes of resonance that were found to exist and these frequencies were dependent on the height of the gas–liquid dispersion and the gas hold-up. Using Eq. (4) as a basis, it can be seen that increasing the dispersion height will result in lower resonance frequencies. Hydrodynamic pressure fluctuations have been reported to occur in the frequency range of order 10 Hz by other researchers [19–21] and this could make identification of the resonance modes harder. To obtain good resolution of resonance frequencies, lower sampling rates are required which would increase the time needed to sample a sufficient amount of the time signal to produce a steady acoustic spectrum. For scales where the diameter of the column is increased then higher resonance modes may exist due to standing waves in the radial direction. These higher modes of resonance would occur at higher frequencies and therefore, if identifiable in the acoustic spectrum, could also be used to follow changes in gas hold-up in columns of larger scale.

Real systems in which foaming and fouling are likely should also be investigated. Foam at the surface of the liquid could affect the boundary conditions for the standing wave.

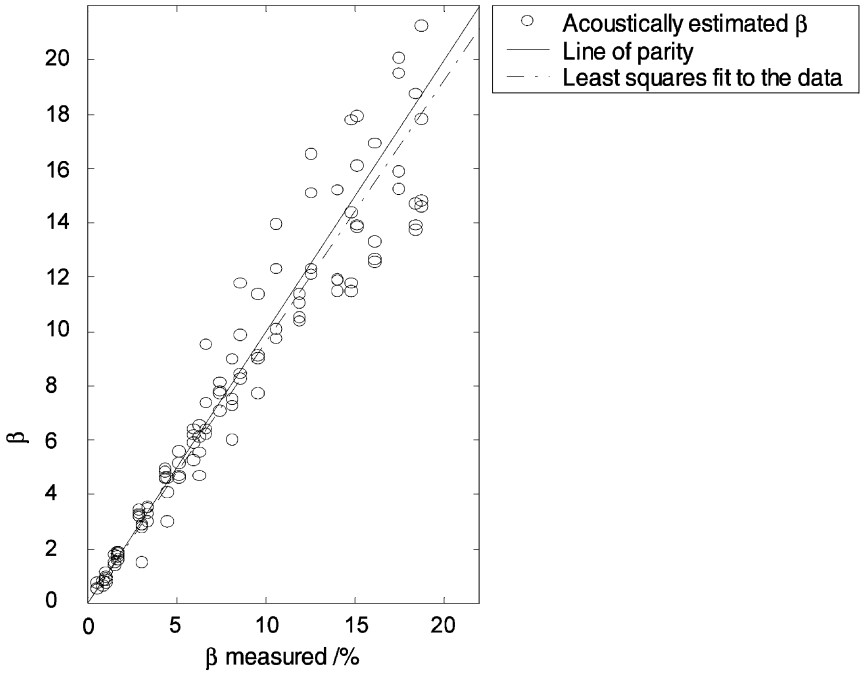

Fig. 7. Parity plot between the gas hold-up estimated from the 2nd to 5th peak frequencies (measured for all experimental conditions) and the gas hold-up measured from the change in the dispersion height.

5. Conclusions

Acoustic emissions in the 0–1000 Hz range were measured inside a laboratory scale bubble column for gas hold-ups up to 20%. The frequencies of peaks in the acoustic emission spectrum corresponded to modal resonance frequencies excited in the column by the sound from bubble formation and consequently were affected by the height of the dispersion and the gas hold-up. There was a very high correlation between the changes in the peak frequencies and the gas hold-up within the bubble column. This technique to monitor gas hold-up could be used in vessels where the dispersion is not visible. Further investigation of the effect of foaming and scale on the acoustic emissions is required to develop the technique for application in real systems.

Acknowledgements

The authors wish to thank the BBSRC for their funding of project 45/E08711 and the Royal Commission of the Exhibition of 1851 for the Dr. Boyd's fellowship.

References

[1] K. van't Riet, J. Tramper, Basic Bioreactor Design, Marcel Dekker, New York, 1991.
[2] G. Kocamustafaogullari, W.D. Huang, J. Razi, Measurement and modeling of average void fraction bubble size and interfacial area, Nucl. Eng. Des. 148 (1994) 437–453.
[3] V.P. Veera, J.B. Joshi, Measurement of gas hold-up profiles in bubble column by Gamma ray tomography: effect of liquid phase properties, Chem. Eng. Res. Des. 73 (A3) (2000) 425–434.
[4] D. Schmitz, D. Mewes, Tomographic imaging of transient multiphase flow in bubble columns, Chem. Eng. J. 77 (1–2) (2000) 99–104.
[5] A.A. Stravs, A. Pittet, U. von Stockar, P.J. Reilly, Measurement of interfacial areas in aerobic fermentations by ultrasonic pulse transmission, Biotechnol. Bioeng. XXVIII (1986) 1302–1309.
[6] L.J. Xu, L.A. Xu, Ultrasound tomography system used for monitoring bubbly gas/liquid two-phase flow, IEEE Trans. Ultrasonics Ferroelect. Frequency Contr. 44 (1) (1997) 67–76.
[7] R. Roy, J.F. Davidson, V.G. Tuponognov, The velocity of sound in fluidised beds, Chem. Eng. Sci. 45 (11) (1990) 3233–3245.
[8] G. Costigan, P.B. Whalley, Measurements of the speed of sound in air–water flows, Chem. Eng. J. 66 (1997) 131–135.
[9] J.W.R. Boyd, J. Varley, The uses of passive measurement of acoustic emissions from chemical engineering processes, Chem. Eng. Sci. 56 (5) (2001) 1749–1767.
[10] M. Minnaert, On musical air-bubbles and the sounds of running water, Philos. Mag. 16 (1933) 235–248.
[11] T.G. Leighton, The Acoustic Bubble, Academic Press, New York, 1994.
[12] J.W.R. Boyd, J. Varley, Sound measurement as a means of gas bubble sizing in aerated agitated tanks, AIChE J. 44 (8) (1997) 1731–1739.
[13] D.P. Koller, P.M. Shankar, Acoustical emissions from bubble clouds, Ultrasonics 32 (3) (1994) 229–233.
[14] S.W. Yoon, L.A. Crum, A. Prosperetti, N.Q. Lu, An investigation of the collective oscillations of a bubble cloud, J. Acoust. Soc. Am. 89 (2) (1991) 700–706.
[15] M. Nicholas, R.A. Roy, L.A. Crum, H. Oguz, A. Prosperetti, Sound emissions by a laboratory bubble cloud, J. Acoust. Soc. Am. 95 (6) (1994) 3171–3182.
[16] N.Q. Lu, A. Prosperetti, S.W. Yoon, Underwater noise emission from bubble clouds, IEEE J. Oceanic Eng. 15 (4) (1990) 275–281.
[17] A.P. Dowling, J.E. Ffowcs Williams, Sound and Sources of Sound, Ellis Horwood, Chichester, UK, 1989.
[18] D.G. Crighton, A.P. Dowling, J.E. Dowling, J.E. Ffowcs Williams, M. Heckl, F.G. Leppington, Modern Methods in Analytical Acoustics, Springer, London, 1992.
[19] J. Drahos, J. Cermak, Diagnostics of gas–liquid flow patterns in chemical engineering systems, Chem. Eng. Process. 26 (1989) 147–164.
[20] C. Vial, E. Camarasa, S. Poncin, G. Wild, N. Midoux, J. Bouillard, Study of hydrodynamic behaviour in bubble columns and external loop airlift reactors through analysis of pressure fluctuations, Chem. Eng. Sci. 55 (2000) 2957–2973.
[21] C. Vial, S. Poncin, G. Wild, N. Midoux, A simple method for regime identification and flow characterisation in bubble columns and airlift reactors, Chem. Eng. Process. 40 (2001) 135–151.